Correlation studies of energy gain and fragmentation in ion-fullerene collisions

J. Opitz,* H. Lebius, B. Saint, S. Jacquet, and B. A. Huber
Département de Recherche Fondamentale sur la Matière Condensée, Service des Ions, des Atomes et des Agrégats, CEA-Grenoble, 17 rue des Martyrs, F-38054 Grenoble Cedex 9, France

H. Cederquist
Atomic Physics, Stockholm University, Frescativägen 24, S-10405 Stockholm, Sweden
(Received 28 September 1998)

Multi-ionization and fragmentation of C_{60} fullerenes induced by collisions with Ar^{8+} ions have been studied in correlation with the energy gain and the number of electrons captured and stabilized by the projectile ion. The method allows us to separate electron capture reactions from transfer ionization processes and to determine the number (r) of active electrons. When one electron is stabilized on the projectile, the target ion C_{60}^{r+} is left intact and the energy gain increases with the charge r, which ranges up to $r=4$. The corresponding mean energy gain values for production of C_{60}^{+} through C_{60}^{4+} are used together with three different models for the electronic response of ionized C_{60} in order to deduce *semiempirical* electron transfer distances for the first four electrons. A model with localized and mobile charges on the surface of the molecule gives a slightly better agreement with earlier measured recoil ion production cross sections than the metal sphere model or an assumption with localized charges kept fixed closest to the projectile during the collisions. The mean energy gain depends on the number of stabilized electrons s. It increases between $s=1$ and 2, then it stays constant, and finally decreases between $s=5$ and 6. The energy distribution for $s=6$ extends to the energy-loss side, which is attributed to close collisions causing a strong electronic excitation of C_{60}. [S1050-2947(99)05405-0]

PACS number(s): 34.70.+e, 61.48.+c

I. INTRODUCTION

Ion-fullerene collisions have attracted great interest during recent years, as they allow one to study the interaction of a charged particle with a multielectron target, characterized by many largely delocalized, nearly equivalent, electrons. Therefore, in addition to phenomena already being observed in ion-atom collisions, collective processes are expected to occur, giving rise to electronic excitation or multi-ionization of the many electron target. In several papers [1–7], dealing with multiply charged ion-C_{60} collisions, the production and stability of multiply charged fullerenes have been discussed. It has been shown that C_{60} can survive in charge states up to 9+ [5] or even up to 10+ [8] at least for several μs. Furthermore, by analyzing the fragmentation spectra in correlation with the projectile charge state [1,6,7], or by evaluating the electron capture cross section as function of the number of stabilized electrons, the first information has been obtained on the relative importance of far and close collisions. Assuming that the fullerene represents a small, thin carbon, foil, one might expect a strong energy loss of the projectile when it penetrates the fullerene cage at a velocity where the electronic stopping power in the solid dominates. Of course this crude picture might be oversimplified due to the finite size of the object. On the other hand, when the multiply charged projectile passes the fullerene at large distances, the electron capture process should be characterized by an energy gain due to the Coulomb repulsion between the two ions in the exit channel.

For collisions of Ar^{8+}, Ar^{13+}, Ar^{14+}, and Ar^{15+} with C_{60} molecules, energy-gain distributions have been measured concerning processes where one or two electrons are stabilized by the projectile [9]. These ΔE spectra were characterized by structured distributions extending to unexpectedly large ΔE values. It was argued that the observed structures are due to the initial transfer of many electrons followed by multiple autoionization processes, leaving only one or two electrons stabilized on the projectile. In Ref. [9], a model for sequential multiple-electron transfer from C_{60} was discussed. It is based on the assumption of localized and mobile charges on the C_{60} molecular ions. Some support for this model was found in the relation between measured total electron-capture cross sections and measured energy gains for pure single-electron capture [9]. At that time, ΔE distributions for a specific number of active electrons had not been measured. Therefore, it was not possible to test this model for more than one active electron. Here, however, such measurements are performed, and in the following we will use mean ΔE values, measured in coincidence with a given recoil charge state, to discuss the electronic response of ionized C_{60}. We use three different models in order to deduce semiempirical mean electron transfer distances for the first four electrons, and compare the results with the transfer distances derived from the corresponding recoil ion production cross sections by Walch *et al.* [1]. The three models are the metal sphere model, the model with localized and mobile charges in the simplified version presented by Selberg *et al.* [9], and a limiting case of the latter in which the localized charges are assumed to be fixed closest to the projectile during the collision.

In the present experiment we have applied the translational energy-gain spectroscopy (TES) [10] in order to mea-

*Present address: Walther-Nernst-Institut, Institut für Physikalische und Theoretische Chemie der Humboldt-Universität zu Berlin, Bunsenstr. 1, D-10017 Berlin, Germany.

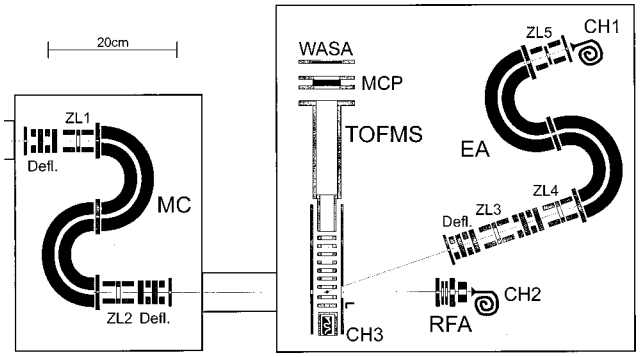

FIG. 1. Schematic view of the experimental setup. Defl: deflection plates; ZL: zoom lenses; MC: energy monochromator; TOFMS: time-of-flight mass spectrometer; CH: channeltron; MCP: multichannelplate, WASA: wedge-and-stripe anode; RFA: retarding field analyzer; EA: energy analyzer.

sure the charge state of the outgoing projectiles in correlation with the mass-to-charge ratio of the produced recoil ions. Thus pure electron-capture reactions can be distinguished from transfer ionization processes, and the energy gain can be studied for nondissociative processes,

$$A^{q+} + C_{60} \rightarrow A^{(q-s)+} + {C_{60}}^{r+} + (r-s)e^- + \Delta E, \qquad (1)$$

as well as for dissociative ones

$$A^{q+} + C_{60} \rightarrow A^{(q-s)+} + {C_{m'}}^{r'+} + {C_{m''}}^{r''+} + \cdots + (r-s)e^- + \Delta E. \qquad (2)$$

In these equations, r denotes the number of active electrons, which are taken away from the fullerene target, s the number of electrons finally stabilized by the projectile ion and r' and r'' $(\Sigma r' = r)$ the charge states of the fragments of masses m' and m''. In the following we will describe some details of the experimental technique before discussing the time-of-flight spectra of the recoil ions and the energy gain spectra measured for projectiles with a given number of stabilized electrons.

II. EXPERIMENTAL TECHNIQUE

The experimental setup is shown in Fig. 1. A beam of multiply charged ions which is delivered by the AIM facility at CEA-Grenoble [11], passes an electrostatic energy analyzer which defines the beam energy within 2 eV per charge. The beam energies are 8 and 16 keV. In the interaction region the ion beam is crossed with a beam of C_{60} molecules, which effuses from a small heated tube (diameter 1 mm) connected to an oven, which is kept at a temperature of 500 °C. Projectile ions which have passed the interaction zone are selected with respect to their scattering angle, and can be analyzed either with a retarding field device with high efficiency or with a high-resolution energy analyzer yielding the charge state and the kinetic energy of the projectile after the collision. Recoil ions are extracted by a weak electrostatic field (15–100 V/cm), and are accelerated in a second field before entering the drift region of a linear Wiley-McLaren time-of-flight (TOF) mass spectrometer, 25 cm in length. Finally, the ions are post-accelerated toward a channel-plate detector biased at a potential of −6 kV in order to increase the detection efficiency. The signals are treated with a fast electronic system allowing for the detection of several fragments and for a registration mode ''event by event.''

The detection efficiency for recoil ions and fragments has been studied in dependence on the extraction field and the post-acceleration voltage. Under the chosen experimental conditions, saturation was obtained for all ions with the exception of C_2^+ fragments. These ions which are formed in superasymmetric fission processes with an appreciable amount of kinetic energy (5–10 eV, depending on the charge state of the decaying fullerene ion) require high extraction fields in order to avoid a ''forward-backward'' structure in the TOF spectrum.

On the one hand, for a given scattering angle θ, energy gain ΔE, and charge state $(q-s)$ of the outgoing projectile, we have measured TOF spectra of ionized fullerenes and fragments. In the normal operation mode a continuous ion beam and a permanent extraction field were used, the projectile ion signal serving as the start and the recoil ion signal as the stop for the time-of-flight measurement. In order to obtain the so-called ''integral recoil ion spectra,'' either the scattering angle or the energy gain can be scanned during the TOF accumulation. These spectra are correlated with a given charge state $(q\text{-}s)$ of the projectile, and an integration over the scattering angle or the energy gain is performed. A ''total recoil spectrum,'' which contains all ions which are produced in the collision process (no correlation with the projectile after the collision), was obtained by pulsing the primary ion beam (width 1 μs, repetition rate 10 kHz) and the extraction field (width 10 μs). In this operation mode, the extraction pulse, which is delayed with respect to the passing ion pulse by about 1 μs, was used as the start signal.

On the other hand, the energy gain spectrum of the projectile correlated with the production of a given intact molecule ${C_{60}}^{r+}$ or fragment ${C_{m'}}^{r'+}$ may also be recorded by setting a time window in the TOF spectrum. In this way, energy-gain spectra for individual processes, characterized by a certain number of active and stabilized electrons, can be measured.

As processes with many active electrons are studied, single-collision conditions have to be ensured. In addition, reactions occurring outside the interaction zone are suppressed due to the presence of an electrostatic potential and an electric field inside the interaction zone. However, the finite width of the ion beam (0.5 mm) and the presence of the extraction field limit the energy resolution in the TES spectra to several eV per charge, depending on the number of stabilized electrons.

III. RESULTS AND DISCUSSION

We have studied the correlation between the energy gain of the charge-state-selected projectile and the recoil TOF spectra for collisions of Ar^{8+} with C_{60} at collision energies of 8 and 16 keV. In particular, we have measured TOF and TES spectra for outgoing Ar projectiles in charge states 7–2, i.e., for cases where 1–6 electrons have been stabilized by the Ar^{8+} projectile.

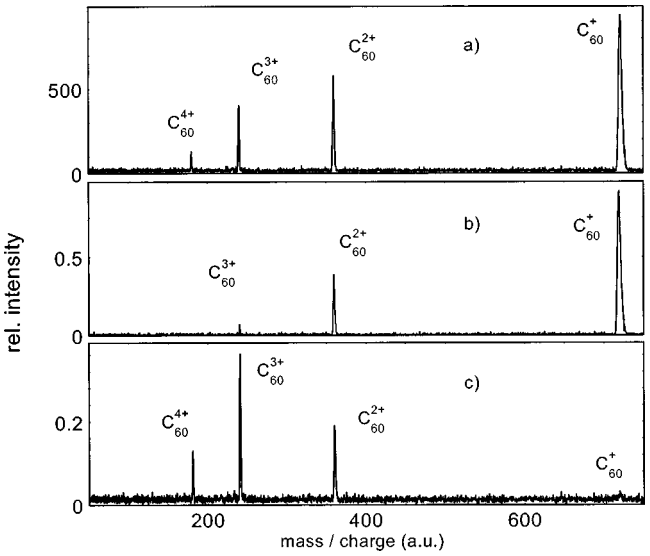

FIG. 2. Mass-charge spectrum of fullerene ions produced in Ar^{8+}/C_{60} collisions, measured in correlation with outgoing Ar^{7+} ions. $E_{ion}=16$ keV; scattering angle $0\pm0.3°$. (a) Integral spectrum (integrated over $\Delta E=-20-100$ eV). (b) $\Delta E=12\pm10$ eV. (c) $\Delta E=36.5\pm10$ eV.

A. Stabilization of one electron ($Ar^{8+}\rightarrow Ar^{7+}$)

Ar^{7+} ions can be produced either in pure single-electron-capture reactions or by transfer ionization processes. In the latter case, several electrons are initially transferred to the projectile but, finally, only one of these is stabilized while the others are lost by Auger processes. Therefore, the TOF spectra measured in correlation with outgoing Ar^{7+} ions may contain C_{60} ions in different charge states. Indeed, as shown in Fig. 2, C_{60} ions are detected in charge states between 1 and 4, which is in agreement with results obtained in Refs. [1,6]. In Fig. 2(a) a mass spectrum (integrated over the energy gain of the projectile) shows that pure single capture is the most dominant process; however, transfer ionization is important as well, yielding an average charge state of the fullerene ion of about 1.5 (this value is somewhat lower than that reported in Ref. [6], which may be due to a different angular acceptance and detection efficiency). The relative intensity of different reaction channels varies with the energy gain ΔE of the projectile. As can be seen in Figs. 2(b) and 2(c) single-electron capture is characterized by rather small energy gains, transfer ionization processes with three or four active electrons occur at larger ΔE values. This is due to the increasing Coulomb repulsion in the exit channel, and the fact that multicapture occurs at smaller internuclear distances. The absence of C_{60-2m} ions, which are due to the emission of C_2 molecules, indicates that the internal temperature of the fullerene ions is rather low, and that these charge states are formed in rather peripheral collisions.

In Fig. 3 we show the kinetic-energy distribution of Ar^{7+} ions which have been measured in coincidence with extracted C_{60}^{+} recoil ions, i.e., they have been produced in pure single-electron-capture reactions. These processes populate dominantly the excited level $n=7$, and with smaller probability the levels $n=5$, 6, and 8, which is in good agreement with the findings at slightly higher energies discussed in Ref. [9]. Furthermore, it is in agreement with theoretical

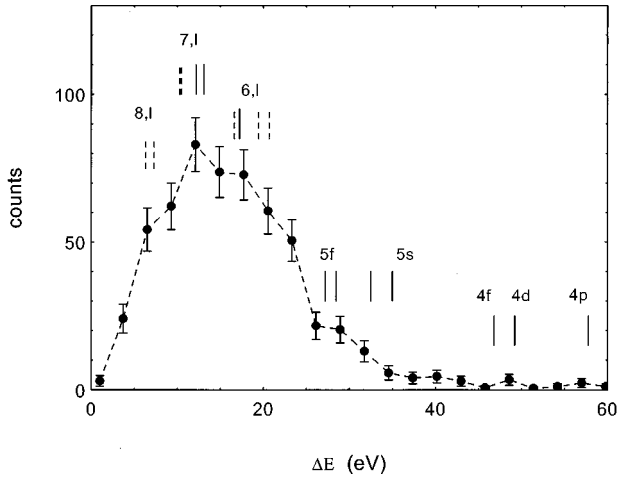

FIG. 3. Energy gain spectrum for Ar^{7+} ions produced in the process $Ar^{8+}+C_{60}\rightarrow Ar^{7+*}(n,1)+C_{60}^{+}+\Delta E$; $E_{ion}=8$ keV. The vertical lines indicate the energy gain for capture into excited levels (full lines from Ref. [12]; dashed lines: extrapolated values).

over-the barrier calculations by Thumm [13]. Due to the limited energy resolution, the structures in the energy gain spectrum, as shown in Ref. [9], are not resolved in the present spectrum.

In a similar way, energy-gain spectra have been obtained for transfer ionization processes by coincidence measurements with C_{60}^{r+} ions in charge states $r=2-4$. The results, which are summarized in Fig. 4, clearly show that the energy gain increases strongly with the number of active electrons. The average ΔE value increases from 12 eV to 23, 32, and about 39 eV when r increases from 1 to 4, respectively. The half-widths of the measured distributions which are partly due to the limited energy resolution amount to ±9.5, ±8.0, ±9.0, and ±13 eV, respectively.

In Table I, we use the presently measured average energy gain values for the processes $Ar^{8+}+C_{60}\rightarrow Ar^{(8-r)+}+C_{60}^{r+}\rightarrow Ar^{7+}+C_{60}^{r+}+(r-s)e^{-}+\Delta E$, with r ranging from 1 to 4, to deduce semiempirical average electron transfer distances. For this we use three different models concerning the

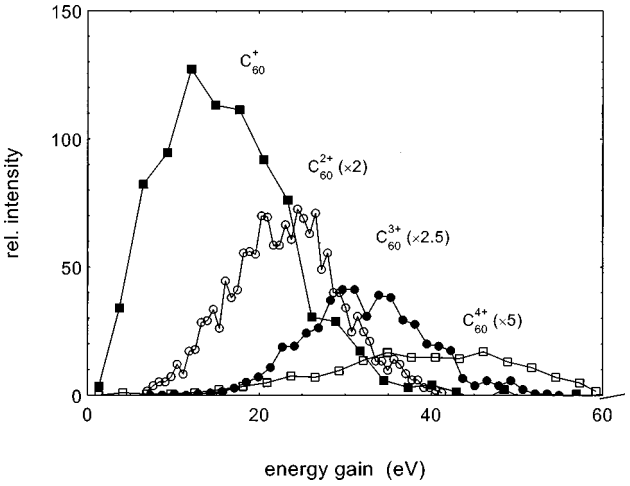

FIG. 4. Energy-gain spectra for Ar^{7+} ions measured in coincidence with C_{60}^{r+} ions in individual charge states $r=1-4$. ($Ar^{8+}+C_{60}$; $E_{ion}=8$ keV).

TABLE I. Energy gain and critical distances for the reaction $Ar^{8+}+C_{60}\rightarrow Ar^{(8-r)+}+C_{60}{}^{r+}\rightarrow Ar^{7+}+C_{60}{}^{r+}+(r-1)e^{-}+\Delta E$. (a) Calculated for a metal sphere without charge localization; (b) determined from absolute electron-capture cross sections (Ref. [1]); (c) the fullerene charge is localized close to the projectile ($6.5a_0$ from the cage center); (d) model of moving localized charges (see Ref. [9]).

Number of active electrons	Charge states		Average energy gain	Critical distance (a_0)			
	$8-r$	r	ΔE (eV)	(a)	(b)	(c)	(d)
1	7	1	12	17.9	22.5	23.4	23.5
2	6	2	23	15.6	20.0	19.7	20.8
3	5	3	32	14.1	17.9	16.5	19.3
4	4	4	39	12.5	16.2	11.9	17.4

charge localization and charge mobility during the collision. The corresponding results are compared with the critical radii deduced by Walch *et al.* [1] from absolute cross sections for producing intact recoil ions $C_{60}{}^{+}$ through $C_{60}{}^{4+}$. The three models are the metal-sphere $C_{60}{}^{r+}$ [dielectric constant $\varepsilon\rightarrow\infty$; (a) in Table I], the full charge $(r+)$ fixed on the projectile side of $C_{60}{}^{r+}$ [column (c)], and a single charge $(1+)$ localized on the projectile side while the remaining charge $(r-1)+$ is assumed to be on the other side of the $C_{60}{}^{r+}$ ion [column (d)]. For the metal sphere model we have used the potentials

$$U_{r-1}(R)=(r-1)(q-r+1)/R+a(q-r+1)^2/(2R^2)-a(q-r+1)^2/(2(R^2-a^2))-Q_{r-1} \quad (3)$$

and

$$U_r(R)=r(q-r)/R+a(q-r)^2/(2R^2)-a(q-r)^2/(2(R^2-a^2))-Q_r, \quad (4)$$

where $a=8.2a_0$ is given by the experimental polarizability α_0, of C_{60} [14], and $\alpha_0=a^3$.

The first term on the right-hand side of Eqs. (3) and (4) corresponds to the Coulomb repulsion between the charges $(r-1)$ and $(q-(r-1))$ [in Eq. (4), r and $(q-r)$], where R is the distance between the projectile and the center of the C_{60} cage. This means that the charge $(r-1)$ is supposed to be equally distributed on the surface of the C_{60} ion, and that the transferred electrons fully screen the projectile charge q. The second and third terms describe the image charge potentials which simulate the effect of polarization. The asymptotic values $(R\rightarrow\infty)$ of the potential curves, which take into account the excitation energy of the final capture states, are denoted by Q_r and Q_{r-1}.

The difference between these asymptotic values is given by the difference of the measured average ΔE values: $\Delta E_r-\Delta E_{r-1}=Q_r-Q_{r-1}$. By setting $U_r=U_{r-1}$ the empirical crossing radii become $R_1=17.9a_0$, $R_2=15.6a_0$, $R_3=14.1a_0$, and $R_4=12.5a_0$ using full screening of the projectile charge.

Assuming instead that the full fullerene charge is located on the molecule surface, closest to the projectile (at a distance $R_0=6.5a_0$ from the center of C_{60}), the potentials become

$$U_{r-1}(R)=(r-1)(q-r+1)/(R-R_0)-\alpha_{r-1}(q-r+1)^2/2R^4-Q_{r-1} \quad (5)$$

and

$$U_r(R)=r(q-r)/(R-R_0)-\alpha_r(q-r)^2/2R^4-Q_r \quad (6)$$

(in the first term, R has been replaced by $R-R_0$). Again we use full screening of the projectile charge. We explicitly include polarization terms in the potentials and, following Selberg *et al.* [9], we scale the polarizability α_r with the ionization potential for $C_{60}{}^{r+}$. This results in larger radii than with the metal sphere model as can be seen in column (c) of Table I.

In the last column of Table I we show the semiempirical capture radii obtained by means of the simplified model with movable and localized charges by Selberg *et al.* [9]. In this version, $a+1$ charge is located on the molecular surface and closest to the projectile during the transfer of the corresponding active electron. When this transfer is completed, the $+1$ charge is assumed to relocate at the far side of the fullerene on a very short-time scale (compared to the collision time). Electron transfer is treated as a sequential process, and the main simplification in Ref. [3] is that the $+1$ charges are all allowed to be at the same position on the far side of C_{60}. This simplifying assumption prevents the positive charges on the molecular surface to arrange themselves to give a realistic representation of the polarization of the charged molecule. It is therefore necessary to include polarization terms in the potentials in the way indicated by Selberg *et al.* [9].

The relevant potential curves which will determine the charge transfer distances thus become

$$U_{r-1,\mathrm{relaxed}}(R)=(r-1)(q-r+1)/(R+R_0)-\alpha_{r-1}(q-r+1)^2/2R^4-Q_{r-1} \quad (7)$$

and

$$U_r(R)=(q-r)/(R-R_0)+(r-1)(q-r)/(R+R_0)-\alpha_r(q-r)^2/2R^4-Q_r, \quad (8)$$

where the term relaxed means that all the positive charge has moved to the far side of the molecule. For the first three radii the agreement is equally good for columns (c) and (d) of Table I. Model (d) gives the best result for R_4.

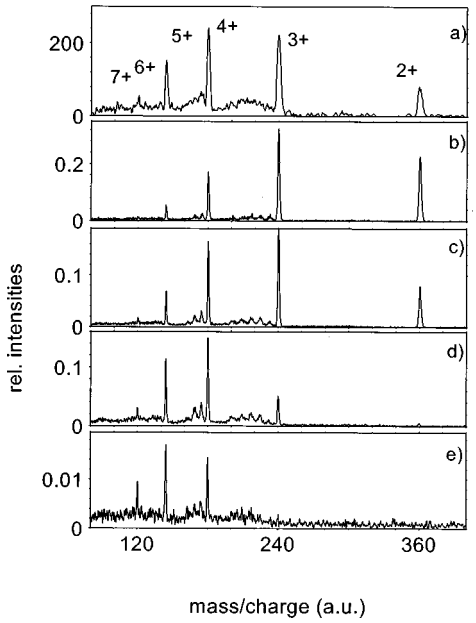

FIG. 5. Mass-charge spectra measured in coincidence with Ar^{6+} ions produced in Ar^{8+}/C_{60} collisions. $E_{ion}=16$ keV. (a) Integral spectrum (integrated over $\Delta E=0-120$ eV). (b) $\Delta E=16\pm10$ eV. (c) $\Delta E=40\pm10$ eV. (d) $\Delta E=64\pm10$ eV. (e) $\Delta E=88\pm10$ eV.

From this part of the work we conclude that the model with localized and mobile charges gives slightly better agreement with the semi-empirical critical distances deduced earlier by Walch *et al.* [1]. However, a definite conclusion from these observations should be taken with care, since we have only discussed average ΔE values from rather wide distributions. Moreover, the critical radii determined from cross-section measurements rely on the absolute cross-section scale which depends on the absolute vapor pressure of C_{60}. Literature values for the latter quantity scatter by about a factor of 2.

B. Stabilization of several electrons ($Ar^{8+}\rightarrow Ar^{6+}\cdots Ar^{2+}$)

1. Time-of-flight spectra

In Fig. 5 the time-of-flight spectrum (integrated over the energy gain) as well as its variation with the energy gain are shown for processes where two electrons have been stabilized by the projectile ion. In contrast to one-electron stabilization processes, pure double-electron capture plays a minor role only. It is more likely, that more than two active electrons are involved. Fullerene ions are produced in charge states between 2 and 7, and the average charge corresponds to 3.7, which means that on the average the numbers of active and stabilized electrons differ by approximately two units. Furthermore, the spectra show fullerene ions which have lost C_2 units, especially for higher charge states ($q\geqslant3$). However, an analysis of coincidences between different fragment ions shows, that these contributions are mainly due to the emission of C_2^+ and C_4^+ ions, and therefore correspond to the decay of parent ions in charge states $q\geqslant4$.

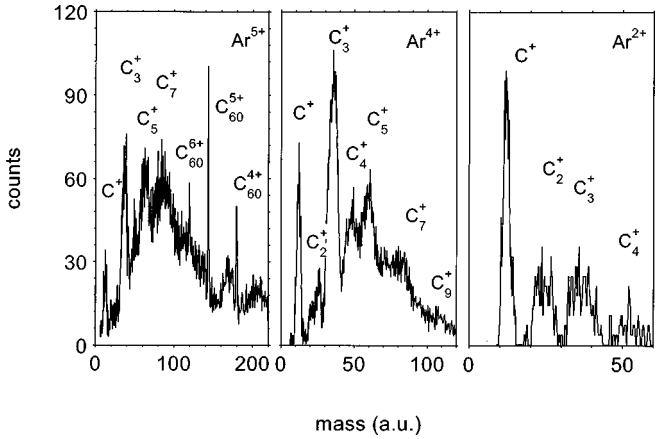

FIG. 6. Integral time-of-flight mass spectra measured in coincidence with outgoing $Ar^{(8-s)+}$ projectiles: $s=3$ (left), $s=4$ (middle), and $s=6$ (right). Collision system: Ar^{8+}/C_{60}; $E_{ion}=16$ keV.

These fission processes, which have been discussed recently by several authors [4,6,7,15–17], will be described in more detail in a forthcoming paper.

Again, processes with a smaller number of active electrons are characterized by lower-energy gains. Thus the maximum in the charge-state distribution shifts from 3+ to 5+ when the energy gain is increased from 30 to 80 eV. It should be mentioned that in the case of two stabilized electrons the spectrum is still dominated by heavy multiply charged fullerene ions. At low-energy-gain values, the abundance of light fragments is nearly negligible. Their relative yield increases with increasing ΔE.

The situation changes when more than two electrons are stabilized. In Fig. 6, integral time-of-flight spectra are shown for the stabilization of 3–6 electrons, i.e., the outgoing projectile is measured in charge states 5–2. In these cases, the spectra are dominated by small, singly charged fragments C_n^+ in the size range $n=1-9$. Smaller fragment sizes become more important with increasing numbers of stabilized electrons, i.e., with the number of active electrons.

In the case of three stabilized electrons (Ar^{5+}), intact fullerene ions in charge states 4, 5, and 6 are present together with a fragment distribution peaking at $n=7(C_7^+)$. Evidently, more than five or six electrons are active, and fragmentation dominates strongly. In the case of coincidences with Ar^{4+} ions, the produced fullerene ions are no longer stable, and only light fragments (dominantly C_3^+ ions) are measured. The spectra shown in Fig. 6 can be compared with results published previously [6]. In both cases the average fragment size decreases with an increasing number of stabilized electrons. Slight differences in the intensity of individual peaks may be due to the low extraction voltage necessary in the present energy-gain experiment.

Finally, an increasing number of stabilized electrons (see the spectrum for Ar^{2+}) yields dominantly C^+ fragments, i.e., is connected with a more or less complete destruction of the fullerene cage. In order to determine whether these processes are due to collisions where the projectile penetrates the fullerene cage or to peripheral collisions, where the cage is destroyed primarily by the excess charge of the produced

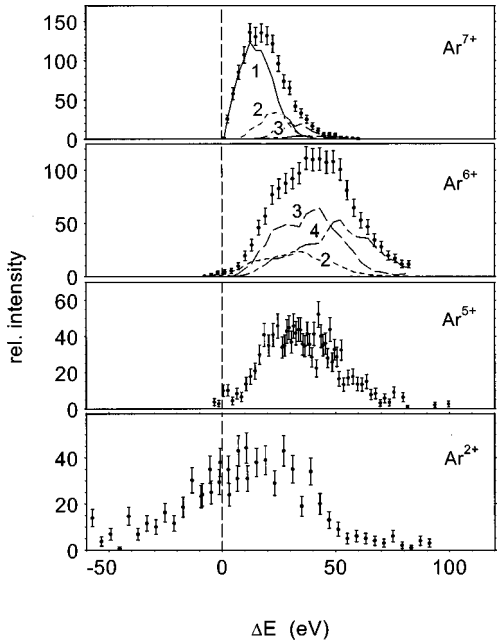

FIG. 7. Energy gain and loss of Ar^{8+} projectiles having stabilized 1–6 electrons in collisions with C_{60}. $E_{ion}=16$ keV. In the case of Ar^{7+} and Ar^{6+} ions the full and dashed lines correspond to $r=1-4$ active electrons.

fullerene ion, the energy gain or loss of these multielectron processes has been studied.

2. Energy gain and energy loss

Figure 7 shows the energy-gain spectra measured in coincidence with the produced recoil ions, and Fig. 8 the average energy gain as a function of $(q-s)$. Processes leading to the stabilization of two electrons are characterized by larger energy gains than those with $s=1$. This is explained by the fact that the C_{60} fullerene loses on the average of 3–4 electrons. According to Table I, these processes are exothermic by about 30–40 eV. For $s=1$ and 2, the full and dashed lines in the energy-gain spectra correspond to individual charge states r of the fullerene ion. If the number of stabilized electrons is further increased (the Ar^{5+} case), the measured energy gain decreases again. On the average 5–8 electrons are active in these reactions. If we neglect electron emission during the collision, i.e., molecular autoionization, and if we assume that captured electrons fully screen the projectile charge, the Coulomb repulsion in the exit channel should decrease again for $r>4$. However, a similar effect may also be related to an increasing electronic excitation of the target. Finally, the energy distribution for outgoing Ar^{2+} projectiles is characterized by a long tail extending to energy losses of about 50 eV. These energy losses are attributed to close collisions which are expected to cause a strong electronic and vibrational excitation of the fullerene ion due to the stopping power of the target. Estimates of the energy loss of argon projectiles in thin carbon foils yield somewhat higher values, which indeed have been measured in similar collision experiments performed at higher collision energies [18,19]. A comparison with those experimental results suggests that, at very low collision energies, penetrating collisions favor a ''neutralization'' of the projectile. For the present collision energies, therefore, we expect larger energy losses for outgoing singly charged Ar^{+} ions or neutral Ar atoms.

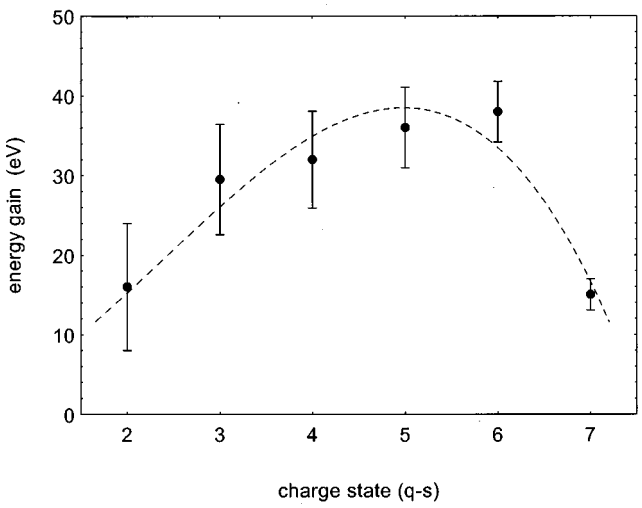

FIG. 8. Average energy defect of electron-capture processes in $Ar^{8+}+C_{60}\rightarrow Ar^{(8-s)+}$ collisions. $E_{ion}=16$ keV. (The dashed line is drawn only to guide the eye.)

IV. SUMMARY

The coincident energy-gain spectroscopy technique has been applied to study low-energy collisions between Ar^{8+} projectiles and C_{60} fullerenes. Time-of-flight recoil-mass spectra have been analyzed for a given charge state and energy gain of the outgoing projectile. Furthermore, kinetic-energy distributions of the projectiles in a given charge state and for a given scattering angle have been measured in coincidence with mass-selected recoil ions.

Secondary Ar^{7+} ions are produced in processes where the fullerene loses up to four electrons. The main process is due to pure single-electron capture which populates dominantly the level $n=7$. From measured energy-gain values, semiempirical electron transfer distances have been deduced and compared to critical capture distances determined from cross-section measurements. The values deduced from a metal sphere model appear to be somewhat low; slightly better agreement is obtained with the model of movable charges, localized on the fullerene surface due to the presence of the projectile ion.

Secondary Ar^{6+} projectiles are formed in processes which are characterized on the average by four active electrons (2–7 electrons). The asymmetric fission represents an important decay process for $q\geqslant 4$; however, the TOF spectra are still dominated by the presence of heavy, multiply charged, fullerene ions.

When more than two electrons are stabilized, the recoil spectrum is dominated by singly charged small-size fragments C_n^{+}, with $n\leqslant 9$. This multifragmentation, which is mainly induced by the excess charge (>6), favors the production of smaller fragments (C^{+}), when the number of stabilized electrons and hence the excess charge is high.

The kinetic energy distribution of outgoing Ar^{2+} projec-

tiles shows a characteristic tail towards energy losses of about 50 eV, which is taken as an indication of close collisions leading to an electronic excitation of the fullerene ion. A comparison of results obtained at different collision energies suggests that ''neutralization'' of the projectile occurs in penetrating collisions, provided that the collision energy is sufficiently low.

ACKNOWLEDGMENTS

These experiments have been performed at the AIM accelerator, a facility of CEA-Grenoble. We gratefully acknowledge the assistance of X. Biquard and F. Gustavo during the preparation of the ion beam.

[1] B. Walch, C. L. Cocke, R. Voelpel, and E. Salzborn, Phys. Rev. Lett. **72**, 1439 (1994).
[2] T. LeBrun, H. G. Berry, S. Cheng, R. W. Dunford, H. Esbensen, D. S. Gemmel, and E. P. Kanter, Phys. Rev. Lett. **72**, 3965 (1994).
[3] H. Shen, P. Hvelplund, D. Mathur, A. Barany, H. Cederquist, N. Selberg, and D. C. Lorents, Phys. Rev. A **52**, 3847 (1995).
[4] S. Cheng, H. G. Berry, R. W. Dunford, H. Esbensen, D. S. Gemmell, E. P. Kanter, and T. LeBrun, Phys. Rev. A **54**, 3182 (1996).
[5] Jian Jin, H. Khemliche, M. H. Prior, and Z. Xie, Phys. Rev. A **53**, 615 (1996).
[6] J. Bernard, L. Chen, A. Denis, J. Desesquelles, and S. Martin, Phys. Scr. **T73**, 286 (1997).
[7] S. Martin, L. Chen, A. Denis, and J. Desesquelles, Phys. Rev. A **57**, 4518 (1998).
[8] A. Brenac, F. Chandezon, H. Lebius, A. Pesnelle, S. Tomita, and B. A. Huber, Phys. Scr. (to be published).
[9] N. Selberg, A. Barany, C. Biedermann, C. J. Setterlind, H. Cederquist, A. Langereis, M. O. Larsson, A. Wännström, and P. Hvelplund, Phys. Rev. A **53**, 874 (1996).
[10] B. A. Huber, Comments At. Mol. Phys. **21**, 15 (1987).
[11] X. Biquard, A. Brenac, F. Gustavo, D. Hitz (unpublished).
[12] C. E. Moore, *Atomic Energy Levels*, Natl. Bur. Stand. U.S. NSRDS No. 35 (U.S. 6 PO, Washington, DC, 1969), p. 224.
[13] U. Thumm, J. Phys. B **27**, 3515 (1994); Phys. Rev. A **55**, 479 (1997).
[14] A. A. Scheidemann, V. V. Kresin, and W. D. Knight, Phys. Rev. A **49**, R4293 (1994).
[15] J. Opitz and B. A. Huber, in *Similarities and Differences Between Atomic Nuclei and Clusters*, edited by Y. Abe, I. Arai, S. M. Lee, and K. Yabana, AIP Conf. Proc. 416 (AIP, New York, 1998), p. 422.
[16] P. Scheier, B. Dünser, and T. D. Märk, Phys. Rev. Lett. **74**, 3368 (1995).
[17] B. Dünser, P. Scheier, and T. D. Märk, Chem. Phys. Lett. **236**, 271 (1995).
[18] S. Martin, J. Bernard, L. Chen, A. Denis, and J. Desesquelles, Phys. Rev. A **59**, R1734 (1999).
[19] M. O. Larsson, P. Hvelplund, M. C. Larsen, H. Shen, H. Cederquist, and H. T. Schmidt, Int. J. Mass Spectrom. Ion Processes **177**, 51 (1998).